Oral Radiol
DOI 10.1007/s11282-015-0203-y

ORIGINAL ARTICLE

Role of diffusion-weighted magnetic resonance imaging in the differentiation of parotid gland tumors

Yasemin Karaman[1] · Anıl Özgür[2] · Demir Apaydın[2] · Cengiz Özcan[3] · Rabia Arpacı[4] · Meltem Nass Duce[2]

Received: 5 September 2014 / Accepted: 14 February 2015

Abstract
Objectives The aim of this study was to assess the role of magnetic resonance diffusion-weighted imaging (DWI) in the characterization of parotid gland tumors using different *b* values.
Methods Thirty-six patients with 41 parotid masses were included in this prospective study. DWI images were obtained using three different *b* values (100, 500, and 1000 s/mm^2). The final diagnosis was made by fine-needle aspiration cytology or histopathological examination. The mean apparent diffusion coefficient (ADC) values of benign lesions versus malignant lesions, pleomorphic adenoma versus Warthin's tumor, pleomorphic adenoma versus malignant lesions, and Warthin's tumor versus malignant lesions were compared using the ADC values obtained with $b = 500$ and $b = 1000$ s/mm^2. When significant differences were found for these comparisons, cutoff points were determined by receiver-operating characteristic curve analysis.
Results The mean ADC value of benign lesions ($n = 32$) was significantly higher than that of malignant lesions ($n = 9$). The mean ADC value of pleomorphic adenoma was significantly higher than that of both Warthin's tumor and malignant tumors. No significant differences between the ADC values of Warthin's tumor and malignant tumors were detected.
Conclusions DWI with both $b = 500$ and $b = 1000$ s/mm^2 may be helpful for the distinction between pleomorphic adenoma and Warthin's tumor, and between pleomorphic adenoma and malignant tumors, but is not efficient for the differentiation of Warthin's tumor from malignant tumors.

Keywords ADC value · Diffusion-weighted imaging · Parotid gland · Parotid tumor

Introduction

Salivary gland tumors account for 3 % of all head and neck tumors, and 80 % of these tumors originate from the parotid gland [1]. Although 1 % of Warthin's tumors undergo malignant transformation, the corresponding rate is about 25 % in pleomorphic adenomas. To reduce local recurrence, a pleomorphic adenoma should be removed with its capsule. While benign tumors are treated with less aggressive surgical approaches, malignant tumors require wide surgical resection. Thus, preoperative diagnosis of the benign or malignant nature of parotid gland tumors is important, because it can change treatment planning.

In recent years, magnetic resonance imaging (MRI) and MRI-based advanced techniques have become the preferred diagnostic tools for differential diagnosis of parotid gland tumors, because of their excellent soft tissue

✉ Anıl Özgür
anilozgur@yahoo.com

1 Department of Radiology, Antalya Education and Research Hospital, Varlık Mahallesi, Kazım Karabekir Caddesi, Muratpaşa, 07030 Antalya, Turkey

2 Department of Radiology, Mersin University Faculty of Medicine, 34. Cadde, Çiftlikköy Kampüsü, 33343 Mersin, Turkey

3 Department of Otorhinolaryngology, Mersin University Faculty of Medicine, 34. Cadde, Çiftlikköy Kampüsü, 33343 Mersin, Turkey

4 Department of Pathology, Mersin University Faculty of Medicine, 34. Cadde, Çiftlikköy Kampüsü, 33343 Mersin, Turkey

Published online: 14 March 2015

resolution, ability for multiplanar imaging, and absence of ionizing radiation [2–5]. Diffusion-weighted imaging (DWI) is one of the advanced techniques and is mainly based on the random motion of water molecules within the voxel. In addition to qualitative analyses, quantitative assessment of diffusion is feasible using apparent diffusion coefficient (ADC) maps. ADC values can be calculated automatically from DWI series and are used in preference to diffusion coefficient values, because diffusion coefficient values can be affected by capillary perfusion, temperature, and magnetic susceptibility. In addition, ADC values can reflect both normal tissue features (extracellular space size, viscosity, cell density, fiber type and density) and tumoral tissue features (tumor cell differentiation level, presence of necrotic or cystic areas, tumor cell density, nucleus/cytoplasm ratio) [2, 6]. High ADC values indicate free motion of water, while low ADC values are indicative of restricted motion. Therefore, the high cellular density of malignant tumors gives rise to low ADC values, whereas high ADC values are calculated for necrotic, fibrotic, and inflamed tissues because of the low density of cellular components. Thus, DWI yields functional data, while MRI provides morphological information. In consideration of the variety and complexity of salivary gland tumors, it can be predicted that DWI may help in the diagnosis, characterization, and differentiation of these tumors.

The aim of this study was to evaluate the efficacy of DWI as a non-invasive technique in the diagnosis and differentiation of parotid gland tumors.

Materials and methods

Forty-one patients who underwent conventional MRI and additional DWI examination between March 2011 and March 2012 for a suspected or known parotid gland mass were prospectively investigated. The local ethical committee approval was obtained to conduct the study and all patients provided written informed consent for the additional DWI examination.

Of the 41 patients, three with sialadenitis and two with parotid gland abscess were excluded from the study. The patients with sialadenitis were diagnosed based on their clinical status and morphological MRI findings. No histopathological/cytopathological assessments were performed for these lesions. Meanwhile, a histopathological diagnosis was available for the patients with parotid gland abscess. Consequently, the final study was conducted with 36 patients (25 males and 11 females). The mean age of the patients was 51.2 years (range 11–87 years). Two patients with Warthin's tumor had more than one lesion, and a total of 41 lesions were evaluated in the study.

All MRI examinations were performed at a 1.5 Tesla MR system (Excite II; General Electric, Milwaukee, WI, USA) using a head and neck coil. The following sequences were obtained: precontrast and postcontrast transverse T1-weighted spin-echo (repetition time/echo time: 659 ms/12 ms; 256 × 192 matrix; 6-mm slice thickness; 1-mm intersection gap; 24 × 24-cm field of view; one signal acquired); sagittal short tau inversion recovery (repetition time/echo time: 5650 ms/35 ms; 256 × 224 matrix; 5-mm slice thickness; 1-mm intersection gap; 32 × 32-cm field of view; 150-ms inversion time; 10 echo-train length); coronal T1-weighted spin-echo (repetition time/echo time: 550 ms/12 ms; 256 × 224 matrix; 5-mm slice thickness; 1-mm intersection gap; 34 × 34-cm field of view; one signal acquired); transverse T2-weighted fast spin-echo (repetition time/echo time: 2875 ms/85 ms; 256 × 192 matrix; 6-mm section thickness; 24 × 24-cm field of view; 15 echo-train length; one signal acquired); and coronal T2-weighted fast spin-echo (repetition time/echo time: 3425 ms/102 ms; 256 × 224 matrix; 5-mm section thickness; 34 × 34-cm field of view; one signal acquired). Contrast-enhanced images were obtained after intravenous injection of 0.1 mmol/kg non-specific gadolinium agent with a delay of about 2 min.

DWI was performed before intravenous contrast agent administration. A multisection spin-echo single-shot echo-planar sequence was used. Sensitizing diffusion gradients were applied sequentially in the x, y, and z directions with b values of 0, 100, 500, and 1000 s/mm^2. The parameters for DWI were as follows: transverse plane; TR: 7125 ms; TE: minimum; field of view: 24 × 24 cm; matrix: 128 × 128; slice thickness: 6 mm; intersection gap: 1 mm; number of excitations: 4.

ADC maps were automatically generated from the DWI sequences using the different b values. ADC values were measured using a circular region of interest of 0.67–0.70 cm^2. Two to six measurements were taken for each lesion and the mean measurement was calculated. The measurements were performed in solid parts of the lesions with restricted diffusion. If there were no areas with restricted diffusion, areas with increased diffusion were used. For heterogeneous lesions, conventional MRI examinations were reviewed and the solid enhanced part of each lesion was considered for measurement. Cystic necrotic parts of the tumors were not included in the measurements. All images were interpreted by consensus by two radiologists with 8 and 5 years of experience in head and neck imaging, respectively.

After conventional MRI and DWI, fine-needle aspiration cytology (FNAC) or surgery was performed in all patients, with the exception of an 11-year-old patient with a previous diagnosis of parotid gland hemangioma. In 15 lesions, the final diagnosis was made by cytopathological analysis

only, because no histopathological specimens were available for patients who did not undergo surgery. In one lesion, the diagnosis was confirmed by histopathological analysis of the surgical specimen. In 24 lesions with both cytopathological and histopathological diagnoses, the histopathological diagnosis was preferred. The ADC values of each lesion were compared with the histopathological/cytopathological data.

Statistical analyses were performed using SPSS 11.5 software (SPSS Inc., Chicago, IL, USA) and MedCalc® v12.7.5 software (MedCalc Software, Ostend, Belgium). The Kolmogorov–Smirnov test was used to compare samples with a reference probability distribution. To determine the significance of differences between benign and malignant lesions, Student's t test was employed. The histopathological findings of the tumors were categorized into three groups. One-way ANOVA was used to compare the mean ADC values among the three groups. Dual comparisons between the three groups were made using Tukey's test. A receiver-operating characteristic (ROC) curve analysis was performed to determine the threshold values. Values of $p < 0.05$ were considered to be statistically significant.

Results

The study included 41 parotid gland tumors with diameters ranging from 10 to 48 mm. Of the 41 lesions, 32 were benign and 9 were malignant. The most common benign and malignant tumors were pleomorphic adenoma (Fig. 1) and lymphoma (Fig. 2), respectively. The histopathological distribution of the lesions and the mean ADC values obtained with the different b values (100, 500, and 1000 s/mm^2) are shown in Table 1.

After the histopathological subtypes were classified, the mean ADC values of benign and malignant lesions were compared. We also made dual comparisons between pleomorphic adenoma versus Warthin's tumor, pleomorphic adenoma versus malignant tumors, and Warthin's tumor versus malignant tumors, because we found significant differences between the mean ADC values of these groups by one-way ANOVA ($p = 0.008$ for $b = 100$; $p < 0.001$ for $b = 500$; $p < 0.001$ for $b = 1000$).

For benign lesions versus malignant lesions, the mean ADC values of benign masses were significantly higher than those of malignant masses for each b value (Table 2). The cutoff points for $b = 100$, $b = 500$, and $b = 1000$ for the differentiation of benign and malignant masses are provided in Table 3.

For pleomorphic adenoma versus Warthin's tumor, there was a significant difference in the mean ADC values for $b = 500$ ($p < 0.001$) and $b = 1000$ ($p < 0.001$), but no significant difference in the values for $b = 100$ ($p = 0.122$) (Fig. 3). The mean ADC value of pleomorphic adenoma was significantly higher than that of Warthin's tumor. The calculated cutoff points for each b value according to the ROC curve analysis, and the sensitivities and specificities of these values are shown in Table 4.

For pleomorphic adenoma versus malignant tumors, the mean ADC values demonstrated significant differences for all b values (Fig. 4). The mean ADC value of pleomorphic adenoma was significantly higher than that of malignant tumors (Table 5). The sensitivities and specificities of the cutoff points based on the ROC curve analysis are shown in Table 6.

For Warthin's tumor versus malignant tumors, there was no significant difference between the ADC values of Warthin's tumor and malignant tumors for all b values. The mean ADC values are shown in Table 7.

The sensitivities and specificities of DWI with both $b = 500$ (Table 8) and $b = 1000$ (Table 9) were similar for the discrimination of the subgroups of parotid tumors. However, $b = 500$ was selected to summarize the findings of our study, and this b value was used for comparisons with the literature based on the minimally higher specificity of $b = 500$ compared with $b = 1000$ in our study.

Discussion

Accurate identification of parotid tumors before surgery is very important, because such characterization can result in completely different management or treatment recommendations. Imaging is one of the essential tools to achieve this identification. MRI is the preferred imaging modality for defining these tumors, as well as for demonstrating the location or extent of the lesions, their perineural/perivascular spread, and the involvement of the facial nerves.

The signal intensity, enhancement pattern, and morphology of the mass are principally interpreted for characterization of a parotid lesion [7, 8]. Christie et al. [9] stated that a poorly defined margin is the only, and most discriminative, feature for predicting malignancy. The T2 signal intensity of a tumor is another remarkable parameter [9, 10]. It was emphasized that T2 hypointensity of a parotid tumor may indicate malignancy, while T2 hyperintensity may reflect a benign nature [7]. On the contrary, some studies stated that the T2 signal intensity did not play a role for predicting the benign or malignant nature of a lesion [8, 11]. Moreover, the signal changes in granulomatous or inflammatory diseases may be confusing. Swartz et al. [12] indicated that the signal characteristics and tumor homogeneity could be correlated with histopathological features. However, tumor homogeneity was not

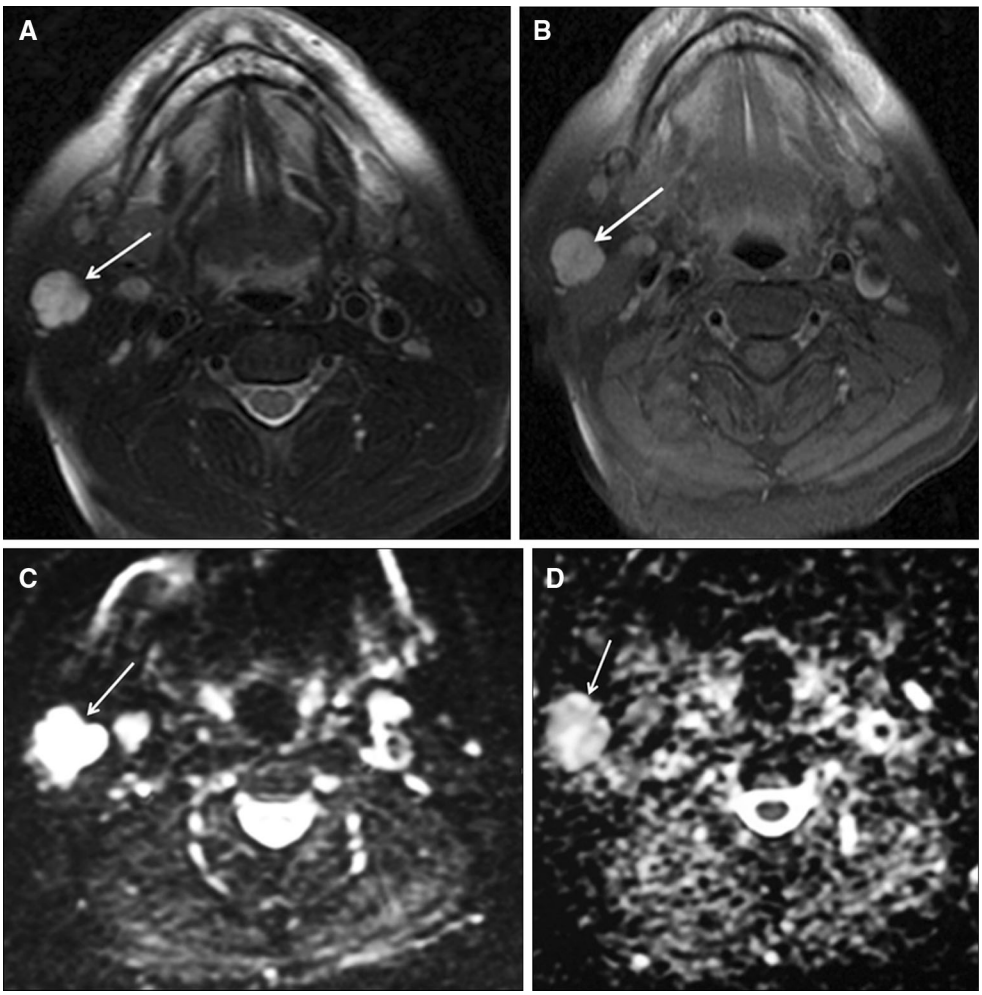

Fig. 1 A 51-year-old male with pleomorphic adenoma in the right parotid gland. **a** The lesion is markedly hyperintense (*arrow*) on a transverse fat-saturated T2-weighted image. **b** Homogeneous and marked enhancement is seen within the lesion (*arrow*) on a postcontrast fat-saturated T1-weighted image. **c** The lesion (*arrow*) shows high signal intensity on DWI. **d** On the corresponding ADC map, the peripheral areas of the tumor (*arrow*) show mild restricted diffusion (mean ADC values in the central and peripheral portions of the lesion are 2.15×10^{-3} and 1.7×10^{-3} mm^2/s, respectively)

found to be consistent with the histopathological findings in another study [11]. Freling et al. [8] reported that tumor margins, homogeneity, and signal intensity did not accurately distinguish benign lesions from malignant lesions. However, infiltration into deep structures, such as the parapharyngeal space, muscles, and bone, can provide a more significant clue for the malignant nature of a lesion. These data suggest that the tumor margins, homogeneity, and signal features may not be sufficient for characterization of most parotid tumors [7, 13–17]. Because more information is needed, specific MRI techniques, such as DWI, MR spectroscopy, and dynamic contrast-enhanced MRI, have become more frequently used for this purpose [18–20]. In the present study, we investigated the diagnostic efficacy of DWI with different b values in the preoperative characterization of parotid gland tumors.

The mean ADC values of benign masses were significantly higher than those of malignant masses for each of the three *b* values examined in our study. In the literature, the ADC values of benign parotid gland tumors were found to be higher than those of malignant tumors in most studies. Thus, it was suggested that ADC values could differentiate between benign and malignant parotid gland tumors [14, 18, 21]. One exception was a study conducted by Matsushima et al. [22], in which no significant difference between the ADC values of 17 benign tumors and 15 malignant tumors was found. Therefore, the authors claimed that ADC values could not be used to differentiate benign and malignant masses.

Several previous studies have calculated cutoff points for benign and malignant masses. In the studies by Wang et al. [18], Srinivasan et al. [23], and Inci et al. [24], the

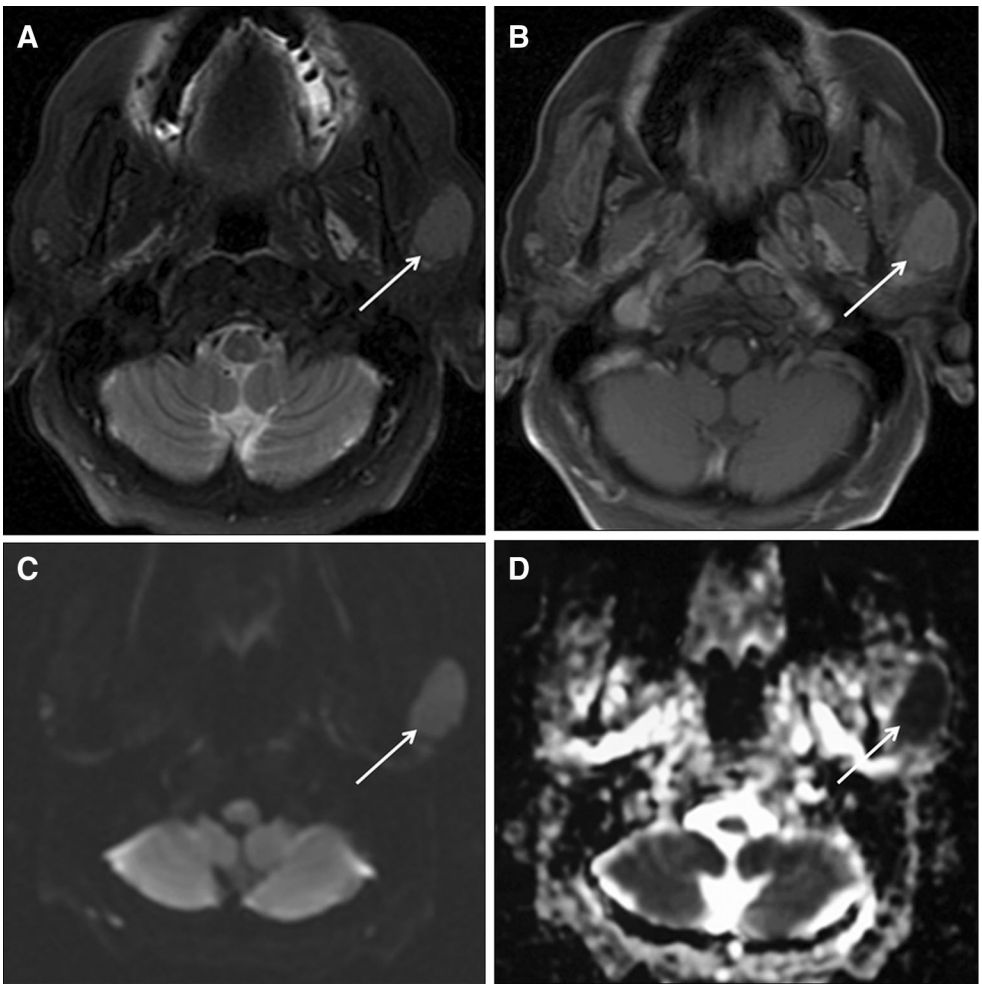

Fig. 2 A 60-year-old female with diffuse large B cell lymphoma. **a** A fat-saturated T2-weighted transverse image shows a well-demarcated hyperintense lesion (*arrow*) in the left parotid gland. **b** A postcontrast fat-saturated T1-weighted image demonstrates mild homogeneous enhancement within the lesion (*arrow*). The lesion (*arrow*) is hyperintense on DWI (**c**) and the corresponding ADC map (**d**) shows marked restricted diffusion (mean ADC value of the lesion is 0.69×10^{-3} mm^2/s)

Table 1 Histopathological diagnoses of lesions and their mean ADC values for different *b* values

Histopathological diagnosis	Mean ADC values ($\times 10^{-3}$ mm^2/s)		
	$b = 100$	$b = 500$	$b = 1000$
Pleomorphic adenoma ($n = 16$)	2.04 ± 0.61	1.88 ± 0.28	1.68 ± 0.28
Warthin's tumor ($n = 13$)	1.59 ± 0.60	1.21 ± 0.40	1.01 ± 0.46
Myoepithelioma ($n = 1$)	1.26	1.70	1.43
Lipoma ($n = 1$)	0.56	0.18	0.13
Hemangioma ($n = 1$)	3.99	3.13	2.80
Small cell lung carcinoma metastasis ($n = 1$)	0.47	0.53	0.45
Adenoid cystic cancer ($n = 1$)	1.30	1.59	1.35
Squamous cell tumor ($n = 3$)	1.92 ± 0.19	1.27 ± 0.30	1.10 ± 0.20
Diffuse large B-cell lymphoma ($n = 4$)	0.88 ± 0.37	0.71 ± 0.14	0.75 ± 0.21

ADC apparent diffusion coefficient, *n* number of lesions

cutoff points were calculated to be 1.22×10^{-3}, 1.3×10^{-3}, and 1.3×10^{-3} mm^2/s, respectively. These cutoff points, obtained with a *b* value of 1000 s/mm^2, were slightly lower than our cutoff point (1.4×10^{-3} mm^2/s), and this can be attributed to several factors. First, the number of malignant tumors was limited in our study.

Table 2 Mean ADC values for different b values of benign and malignant lesions

b values	Parotid lesions	Mean ADC values ($\times 10^{-3}$ mm^2/s)	p
100	Benign lesions ($n = 32$)	1.85 ± 0.76	0.031
	Malignant lesions ($n = 9$)	1.23 ± 0.61	
500	Benign lesions ($n = 32$)	1.59 ± 0.58	0.004
	Malignant lesions ($n = 9$)	0.98 ± 0.41	
1000	Benign lesions ($n = 32$)	1.38 ± 0.59	0.026
	Malignant lesions ($n = 9$)	0.90 ± 0.32	

ADC apparent diffusion coefficient, *n* number of lesions

Table 3 Sensitivities, specificities, and cutoff points with different b values for the differentiation of benign tumors from malignant tumors

	$b = 100$	$b = 500$	$b = 1000$
AUC	0.74	0.82	0.76
Cutoff point according to ADC value ($\times 10^{-3}$ mm^2/s)	1.8	1.6	1.4
Sensitivity [95 % confidence interval]	88.9 [51.8–99.7]	100 [66.4–100]	100 [66.4–100]
Specificity [95 % confidence interval]	56.3 [37.7–73.6]	53.1 [34.7–70.9]	51.6 [33.1–69.8]

AUC area under curve, *ADC* apparent diffusion coefficient

Second, malignant tumors were not a unique group, and there were several tumor types with different degrees of differentiation and structural differences that might have affected the ADC values. These facts might have contributed to the discrepancy between the cutoff points. The higher cutoff point (1.6×10^{-3} mm^2/s) for $b = 500$ in our study is understandable, because the ADC values calculated from low b value images are expected to be higher than those calculated from high b value images.

We do not know why the diagnostic accuracy of DWI using $b = 500$ was similar (even better in means of specificity) to that using $b = 1000$. However, these findings may provide valuable data for clinical practice. MR images obtained with high b values, such as $b = 1000$ s/mm^2, may be of low quality because of artifacts, which may preclude calculation of ADC values of the lesion [18]. In such cases, ADC values calculated for $b = 500$ may be confidently used for the discrimination of parotid lesions. Conversely, ADC values obtained with low b values (0 and 100 s/mm^2) have limited diagnostic utility, because they contain a considerable effect of perfusion rather than the diffusion weight.

In our study, the mean ADC value of pleomorphic adenoma was calculated to be $1.86 \pm 0.28 \times 10^{-3}$ mm^2/s for $b = 500$, which was consistent with the literature. In the studies by Motoori et al. [4] and Eida et al. [2], it was indicated that pleomorphic adenomas with rich chondroid and myxoid matrix showed high ADC values. In almost all of our pleomorphic adenoma cases, the histopathological analyses revealed a myxoid stromal component in the tumors, which might explain the high ADC values.

In our study, the mean ADC value of pleomorphic adenoma was significantly higher than that of Warthin's tumor ($1.21 \pm 0.4 \times 10^{-3}$ mm^2/s) and malignant tumors ($0.98 \pm 0.41 \times 10^{-3}$ mm^2/s), with high sensitivity and specificity of the calculated cutoff points. Warthin's tumor behaves less aggressively than pleomorphic adenoma and malignant tumors [25, 26]. Despite treatment by enucleation, the recurrence rate remains low [25]. Thus, preoperative differentiation of Warthin's tumor from pleomorphic adenoma and malignant tumors is valuable. In the study by Inci et al. [24], the mean ADC value of pleomorphic adenoma was higher than that of Warthin's tumor and malignant tumors. Yerli et al. [27] found that the mean ADC value of Warthin's tumor was significantly lower than that of pleomorphic adenoma. In the study by Habermann et al. [26], which included 43 pleomorphic adenomas among 136 primary parotid gland masses, the authors concluded that pleomorphic adenoma was distinguishable from all other tumors by its ADC values. Consistent with this prior study, Yoshino et al. [5] found that the mean ADC values of pleomorphic adenoma and Warthin's tumor were 1.99×10^{-3} and 0.89×10^{-3} mm^2/s, respectively. In the studies by Ikeda et al. [13], Yoshino et al. [5], and Habermann et al. [26], the mean ADC values of Warthin's tumor were low and similar ($0.85 \pm 0.14 \times 10^{-3}$–$0.96 \pm 0.13 \times 10^{-3}$ mm^2/s). Ikeda et al. [13] also concluded that the mean ADC value of Warthin's tumor was significantly lower than that of malignant tumors. On the contrary, Yerli et al. [14] suggested that there was no significant difference between the mean ADC values of Warthin's tumor and malignant tumors.

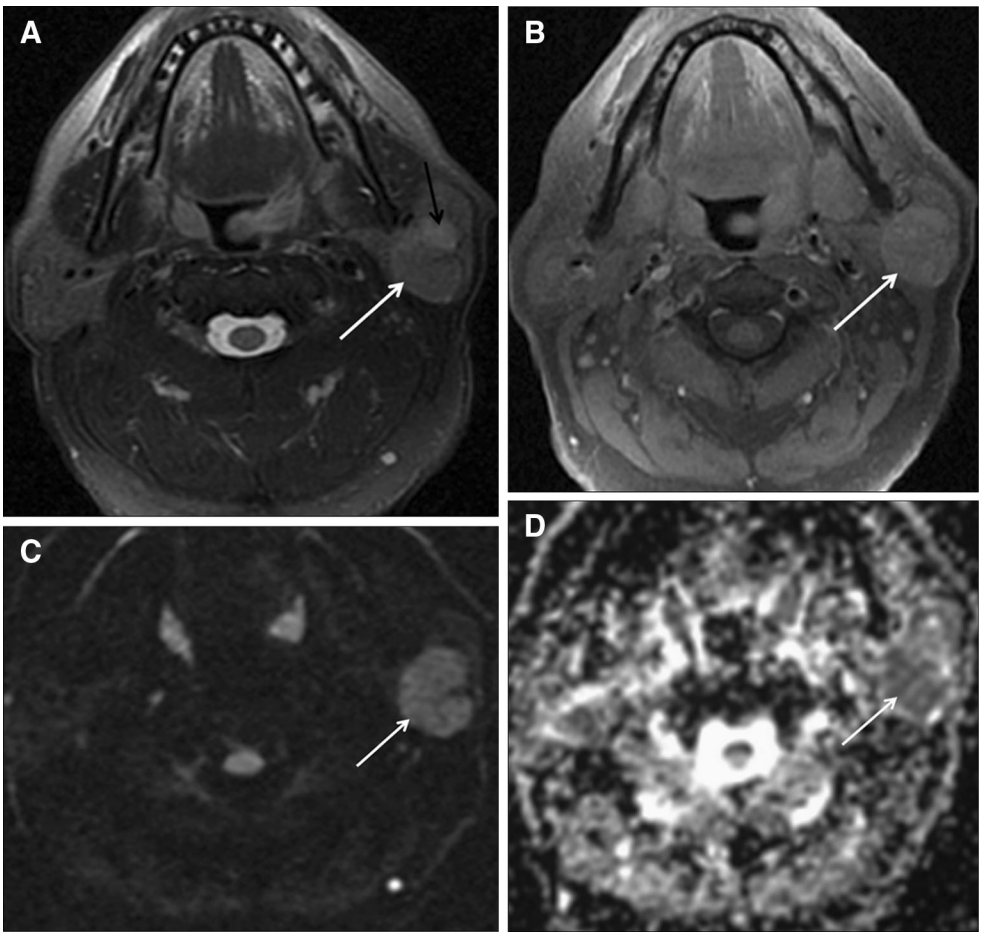

Fig. 3 A 53-year-old male with Warthin's tumor within the right parotid gland. **a** The lesion (*white arrow*) is slightly hyperintense on a transverse fat-saturated T2-weighted image. Note the nodular-shaped hyperintense area in the anterior portion of the lesion, which may represent a cystic component (*black arrow*). **b** The solid component of the lesion (*arrow*) shows mild to moderate enhancement on a fat-saturated T1-weighted postcontrast image. The solid component of the lesion (*arrow*) shows high signal intensity on DWI (**c**) and the corresponding ADC map (**d**) shows restricted diffusion (mean ADC value is 0.93×10^{-3} mm^2/s)

Table 4 Sensitivities, specificities, and cutoff points with different *b* values for the differentiation of pleomorphic adenoma from Warthin's tumor

	$b = 500$	$b = 1000$
AUC	0.90	0.88
Cutoff point according to ADC value ($\times 10^{-3}$ mm^2/s)	1.5	1.1
Sensitivity [95 % confidence interval]	84 [54.6–98.1]	84.6 [54.6–98.1]
Specificity [95 % confidence interval]	93.7 [69.8–99.8]	93.3 [68.1–99.8]

AUC area under curve, *ADC* apparent diffusion coefficient

They explained this finding by the fact that the majority of their malignant tumors were cases of lymphoma. Similarly, we did not find any significant difference between the ADC values of Warthin's tumor and malignant tumors. We think that this finding arose because lymphoma accounted for a large proportion (4/9) of our malignant tumors, similar to the case for Yerli et al. [14].

In our study, the malignant group was mostly composed of secondary tumors of the parotid gland, of which four were lymphoma, one was a metastasis of small cell lung carcinoma, and three were local invasion or metastasis of squamous cell carcinoma, and only one lesion was a primary adenoid cystic carcinoma of the parotid gland. The ADC value of the adenoid cystic carcinoma was 1.59×10^{-3} mm^2/s. This was the highest ADC value among the malignant lesions and was similar to the ADC values of benign tumors. In this case, no clinical suspicion favoring malignancy was present. Moreover, the FNAC

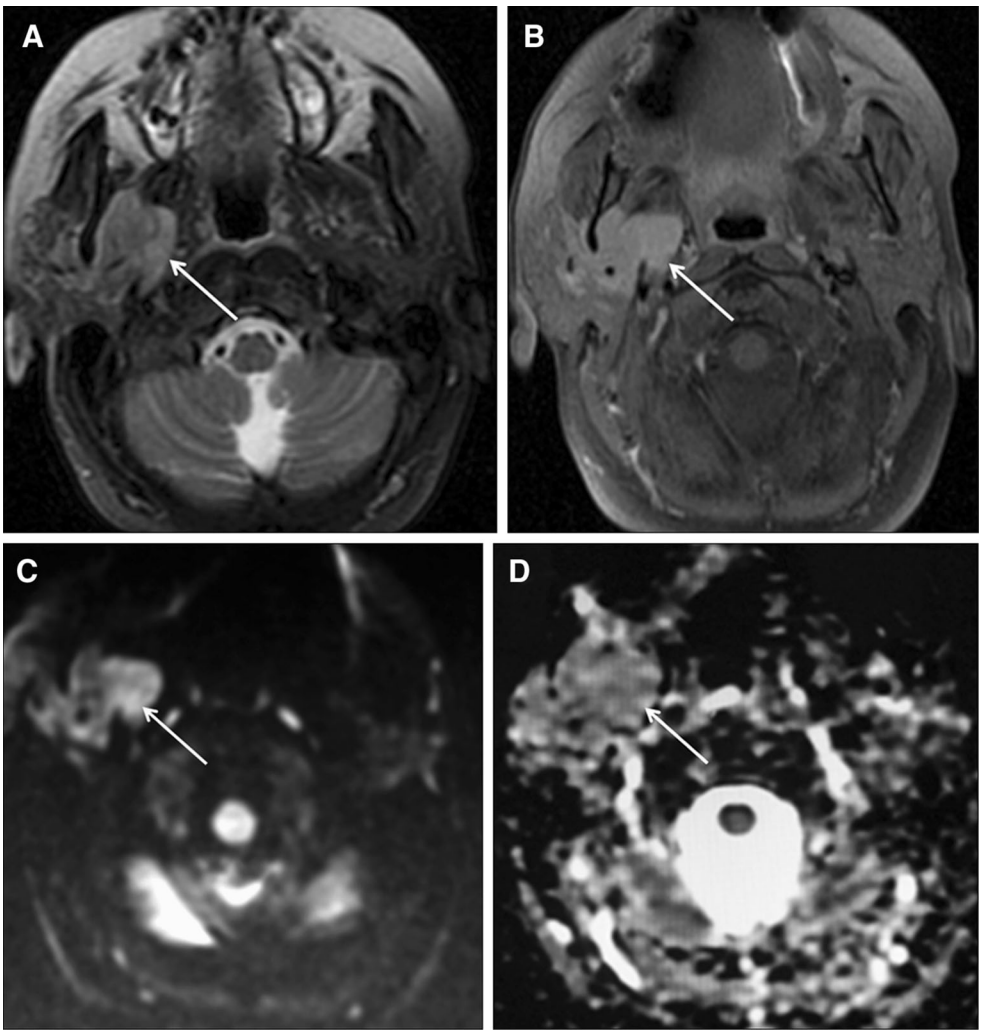

Fig. 4 A 45-year-old female with a solid lesion in the deep lobe of the right parotid gland, infiltrating the adjacent structures and encasing the vessels. Although the initial cytopathological diagnosis was pleomorphic adenoma, the final histopathological examination revealed adenoid cystic carcinoma. **a** The lesion (*arrow*) is hyperintense on a transverse fat-saturated T2-weighted image. **b** A postcontrast fat-saturated T1-weighted image reveals homogeneous and marked enhancement within the lesion (*arrow*). The tumor (*arrow*) shows slightly high signal intensity on DWI (**c**) and the corresponding ADC map (**d**) shows restricted diffusion (mean ADC value is 1.58×10^{-3} mm^2/s)

Table 5 Mean ADC values of pleomorphic adenoma and malignant tumors

b values	Parotid lesions	Mean ADC values ($\times 10^{-3}$ mm^2/s)	*p*
100	Pleomorphic adenoma	2.04 ± 0.61	0.008
	Malignant tumors	1.23 ± 0.61	
500	Pleomorphic adenoma	1.88 ± 0.28	<0.001
	Malignant tumors	0.98 ± 0.41	
1000	Pleomorphic adenoma	1.68 ± 0.32	<0.001
	Malignant tumors	0.90 ± 0.32	

ADC apparent diffusion coefficient

result was pleomorphic adenoma. However, on conventional MRI sequences, the lesion, which was located in the deep lobe, was found to invade the superficial lobe and parapharyngeal space and encase the vascular structures. These findings raised the suspicion of malignancy preoperatively. In the study by Matsushima et al. [22], the mean

Table 6 Sensitivities, specificities, and cutoff points with different b values for the differentiation of pleomorphic adenoma from malignant tumors

	$b = 100$	$b = 500$	$b = 1000$
AUC	0.85	0.96	0.95
Cutoff point according to ADC value ($\times 10^{-3}$ mm^2/s)	1.8	1.6	1.4
Sensitivity [95 % confidence interval]	88.9 [51.8–99.7]	100 [66.4–100]	100 [66.4–100]
Specificity [95 % confidence interval]	81.3 [54.4–96]	81.3 [54.4–96]	80 [51.9–95.7]

AUC area under curve, *ADC* apparent diffusion coefficient

Table 7 Mean ADC values of Warthin's tumor and malignant tumors

b values	Parotid lesions	Mean ADC values ($\times 10^{-3}$ mm^2/s)	p
100	Warthin's tumor	1.59 ± 0.6	0.374
	Malignant tumors	1.23 ± 0.61	
500	Warthin's tumor	1.21 ± 0.4	0.293
	Malignant tumors	0.98 ± 0.41	
1000	Warthin's tumor	1.01 ± 0.46	0.762
	Malignant tumors	0.90 ± 0.32	

ADC apparent diffusion coefficient

Table 8 Sensitivities, specificities, cutoff points, and discrimination values of DWI for $b = 500$

$b = 500$	Discrimination	Cutoff point ($\times 10^{-3}$)	Sensitivity (%)	Specificity (%)
Benign lesions versus malignant lesions	+	1.6	100	53
Pleomorphic adenoma versus Warthin's tumor	+	1.5	84	93.7
Pleomorphic adenoma versus malignant tumors	+	1.6	100	81
Warthin's tumor versus malignant tumors	−			

Table 9 Sensitivities, specificities, cutoff points, and discrimination values of DWI for $b = 1000$

$b = 1000$	Discrimination	Cutoff point ($\times 10^{-3}$)	Sensitivity (%)	Specificity (%)
Benign lesions versus malignant lesions	+	1.4	100	51.6
Pleomorphic adenoma versus Warthin's tumor	+	1.1	84.6	93.3
Pleomorphic adenoma versus malignant tumors	+	1.4	100	80
Warthin's tumor versus malignant tumors	−			

ADC values of four adenoid cystic carcinoma were higher than those of all malignant lesions and the mean ADC value of adenoid cystic carcinoma overlapped with that of pleomorphic adenoma.

We found that the mean ADC value of lymphomas was $0.71 \pm 0.14 \times 10^{-3}$ mm^2/s, which was lower than the mean ADC value of malignant tumors. This was consistent with the literature [2, 18, 24]. More abundant macromolecular proteins, as well as reduced extracellular space because of high cellularity, are speculated to reduce the ADC values in lymphomas [28]. The ADC value of the metastatic small cell carcinoma was even lower than that of lymphomas (0.5×10^{-3} mm^2/s for $b = 500$). As with lymphoma, this finding might be related to the homogeneity and increased cellularity of the tumor.

There were three cases of metastatic/invasive squamous cell carcinoma to the parotid gland in our malignant group. The ADC values of these cases were 1.61×10^{-3}, 1.07×10^{-3}, and 1.12×10^{-3} mm^2/s, respectively, and were not unique. Conventional MRI findings, such as contour irregularity, invasion of the superficial parotid lobe and parapharyngeal space, and suspicious involvement of adjacent structures, were helpful for predicting the malignant nature of these tumors, rather than the ADC values.

There was a lipoma in the study group. The mean ADC values of this single case of lipoma were lower than those

of all malignant lesions at $b = 500$ and $b = 1000$. These findings are consistent with the literature, because two previous studies found overlapping low ADC values between malignant tumors and lipomas [26, 27]. The low ADC values of lipoma may influence the cutoff points for the discrimination of benign and malignant lesions, and this may be a drawback of the present study. However, although malignant tumors and lipomas have overlapping low ADC values, the typical MRI signal features of lipoma enable a correct diagnosis [27].

Our study had some limitations. First, because of the small sizes of the lesions, the ADC measurements were not optimal in some tumors. Second, in lesions with heterogeneous architectures, the ADC values were obtained from enhanced solid parts. However, because of the unavoidable small sizes of these areas, the measurements might have been suboptimal and not representative of the whole lesions. The third limitation was the relatively limited number and variety of malignant cases, compared with Warthin's tumor and pleomorphic adenoma cases, which in turn affected the statistical analyses. For this reason, we could not make comparisons between the subgroups of malignant lesions. However, the incidence of malignant parotid tumors is not high in general, and a similar limitation was also valid for other studies in the literature.

In conclusion, DWI and ADC measurements obtained with two different b values (500 and 1000 s/mm^2) can add more information to the differentiation of malignant and benign parotid tumors. DWI may be helpful in the distinction between pleomorphic adenoma and Warthin's tumor, and between pleomorphic adenoma and malignant tumors because the mean ADC value of pleomorphic adenoma is significantly higher than that of Warthin's tumor and malignant tumors. However, DWI is not useful for differentiating Warthin's tumor from malignant tumors because of the overlapping mean ADC values of these two subgroups.

Conflict of interest Yasemin Karaman, Anıl Özgür, Demir Apaydın, Cengiz Özcan, Rabia Arpacı, and Meltem Nass Duce declare that they have no conflict of interest.

Human rights statement All procedures followed were in accordance with the ethical standards of the responsible committee on human experimentation (institutional and national) and with the Helsinki Declaration of 1964 and later versions.

Informed consent Informed consent was obtained from all patients for being included in the study.

References

1. Som PM, Curtin HD. Head and neck imaging. 4th ed. St. Louis: Mosby; 2003.
2. Eida S, Sumi M, Sakihama N, Takahashi H, Nakamura T. Apparent diffusion coefficient mapping of salivary gland tumors: predictions of the benignancy and malignancy. AJNR Am J Neuroradiol. 2007;28:116–21.
3. Habermann CR, Gossrau P, Graessner J, Arndt C, Cramer MC, Reitmeier F, et al. Diffusion-weighted echo-planar MRI: a valuable tool for differentiating primary parotid gland tumors? Rofo. 2005;177:940–5.
4. Motoori K, Yamamoto S, Ueda T, Nakano K, Muto T, Nagai Y, et al. Inter- and intratumoral variability in magnetic resonance imaging of pleomorphic adenoma: an attempt to interpret the variable magnetic resonance findings. J Comput Assist Tomogr. 2004;28:233–46.
5. Yoshino N, Yamada I, Ohbayashi N, Honda E, Ida M, Kurabayashi T, et al. Salivary glands and lesions: evaluation of apparent diffusion coefficient with split-echo diffusion-weighted MR imaging-initial results. Radiology. 2001;221:837–42.
6. Szafer A, Zhong J, Anderson AW, Gore JC. Diffusion-weighted imaging in tissues: theoretical models. NMR Biomed. 1995;8:289–96.
7. Yousem DM, Kraut MA, Chalian AA. Major salivary gland imaging. Radiology. 2000;216:19–29.
8. Freling NJ, Molenaar WM, Vermey A, Mooyaart EL, Panders AK, Annyas AA, et al. Malignant parotid tumors: clinical use of MR imaging and histologic correlation. Radiology. 1992;185:691–6.
9. Christe A, Waldherr C, Hallett R, Zbaeren P, Thoeny H. MR imaging of parotid tumors: typical lesion characteristics in MR imaging improve discrimination between benign and malignant disease. AJNR Am J Neuroradiol. 2011;32:1202–7.
10. Som PM, Biller HF. High grade malignancies of the parotid gland: identification with MR imaging. Radiology. 1989;73:823–6.
11. Teresi LM, Lufkin RB, Wortham DG, Abemayor E, Hanafee WN. Parotid masses: MR imaging. Radiology. 1987;163:405–9.
12. Swartz JD, Rothman MI, Marlowe FI, Berger AS. MR imaging of parotid mass lesions: attempts at histopathologic differentiation. J Comput Assist Tomogr. 1989;13:789–96.
13. Ikeda M, Motoori K, Hanazawa T, Nagai Y, Yamamoto S, Ueda T, et al. Warthin tumor of parotid gland: diagnostic value of MR imaging with histopathologic correlation. AJNR Am J Neuroradiol. 2004;25:1256–62.
14. Yerli H, Ağıldere AM, Aydın E, Geyik E, Haberal N, Kaskati T, et al. Value of apparent diffusion coefficient calculation in the differential diagnosis of parotid gland tumors. Acta Radiol. 2007;48:980–7.
15. Alibek S, Zenk J, Bozzato A, Lell M, Grunewald M, Anders K, et al. The value of dynamic MRI studies in parotid tumors. Acad Radiol. 2007;14:701–10.
16. Howlett DC, Kesse KW, Hughes DV, Sallomi DF. The role of imaging in the evaluation of parotid disease. Clin Radiol. 2002;57:692–701.
17. Ikeda K, Katoh T, Ha-Kawa SK, Iwai H, Yamashita T, Tanaka Y. The usefulness of MR in establishing the diagnosis of parotid pleomorphic adenoma. AJNR Am J Neuroradiol. 1996;17:555–9.
18. Wang J, Takashima S, Takayama F, Kawakami S, Saito A, Matsushita T, et al. Head and neck lesions: characterization with diffusion-weighted echo-planar MR imaging. Radiology. 2001;220:621–30.
19. Yabuuchi H, Fukuya T, Tajima T, Hachitanda Y, Tomita K, Koga M. Salivary gland tumors: diagnostic value of gadolinium-enhanced dynamic MR imaging with histopathologic correlation. Radiology. 2003;226:345–54.
20. King AD, Yeung DK, Ahuja AT, Tse GM, Yuen HY, Wong KT, et al. Salivary gland tumors at in vivo proton MR spectroscopy. Radiology. 2005;237:563–9.
21. White ML, Zhang Y, Robinson RA. Evaluating tumors and tumor-like lesions of the nasal cavity, the paranasal sinuses, and the

adjacent skull base with diffusion-weighted MRI. J Comput Assist Tomogr. 2006;30:490–5.
22. Matsushima N, Maeda M, Takamura M, Takeda K. Apparent diffusion coefficients of benign and malignant salivary gland tumors: comparison to histopathological findings. J Neuroradiol. 2007;34:183–9.
23. Srinivasan A, Dvorak R, Perni K, Rohrer S, Mukherji SK. Differentiation of benign and malignant pathology in the head and neck using 3T ADC values: early experience. AJNR Am J Neuroradiol. 2008;29:40–4.
24. Inci E, Hocaoğlu E, Kılıçkesmez O, Aydın S, Timilli C. Quantitative diffusion-weighted MR imaging in the differential diagnosis of parotid gland tumors: is it a useful technique? Türkiye Klinikleri J Med Sci. 2010;30:1339–45.
25. Heller KS, Attie JN. Treatment of Warthin's tumor by enucleation. Am J Surg. 1988;156:294–6.
26. Habermann CR, Arndt C, Graessner J, Diestel L, Peterson KU, Reitmeier F, et al. Diffusion-weighted echo-planar MR imaging of primary parotid gland tumors: is a prediction of different histologic subtypes possible? AJNR Am J Neuroradiol. 2009;30:591–6.
27. Yerli H, Aydın E, Haberal N, Harman A, Kaskati T, Alibek S. Diagnosing common parotid tumours with magnetic resonance imaging including diffusion-weighted imaging vs fine needle aspiration cytology: a comparative study. Dentomaxillofac Radiol. 2010;39:349–55.
28. AbdelRazek AA, Soliman NY, Elkhamary S, Alsharaway MK, Tawfik A. A role of diffusion-weighted MR imaging in cervical lymphadenopathy. Eur Radiol. 2006;16:1468–77.